Tetrahedron 75 (2019) 2778–2784

Contents lists available at ScienceDirect

Tetrahedron

journal homepage: www.elsevier.com/locate/tet

The structure and racemization of 1,2-bis(pentaphenylphenyl) benzene

Ha Thuy Thanh Nguyen [a], Joel T. Mague [a], Qi Zhao [a], Christina M. Kraml [b], Neal Byrne [b], Robert A. Pascal Jr. [a, *]

[a] Department of Chemistry, Tulane University, New Orleans, LA 70118, USA
[b] Lotus Separations LLC, Princeton, NJ 08544, USA

ARTICLE INFO

Article history:
Received 1 March 2019
Accepted 28 March 2019
Available online 2 April 2019

Keywords:
Polyphenyl aromatics
Cyclopentadienones
Alkynes
Dynamic NMR spectroscopy

ABSTRACT

1,2-Bis(pentaphenylphenyl)benzene (**2**) was synthesized by the cycloaddition of 1,2-bis(phenylethynyl) benzene and tetracyclone. Its X-ray structure was determined, and the molecule adopts a C_2-symmetric conformation in the crystal. Monomethoxy and dimethoxy derivatives of compound **2** were also prepared, and dynamic NMR studies of these compounds yielded a free energy of activation for racemization ($\Delta G^{\ddagger}_{rac}$) of 20.3 kcal/mol at 423 K. The results are compared with estimates of $\Delta G^{\ddagger}_{rac}$ for **2** by various DFT methods.

1. Introduction

A decade ago we examined the conformational reactions of 1,3,5-tris(pentaphenylphenyl)-benzene (**1**) by both experimental and computational methods [1]. Of particular interest was the possibility that this large, D_3-symmetric molecular propeller might be configurationally stable and resolvable. At each level of theory employed for the computational studies, the lowest energy pathway for racemization proceeds through a C_{3h}-symmetric transition state structure, with the following calculated free energies of racemization ($\Delta G^{\ddagger}_{rac}$): AM1 [2], 18.9 kcal/mol; HF/STO-3G [3], 23.6 kcal/mol; and B3LYP/6-31G(d) [4], 20.8 kcal/mol [1]. The experimental $\Delta G^{\ddagger}_{rac}$ was then determined to be 20.8 kcal/mol by dynamic chromatography [1,5], in perfect agreement with the B3LYP calculations.

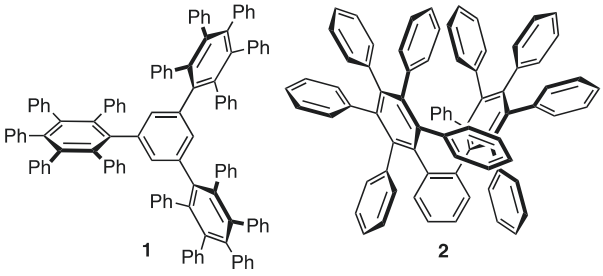

Would a more highly congested, chiral, polyphenyl aromatic hydrocarbon be resolvable? 1,2-Bis(pentaphenylphenyl)benzene (**2**) is a possibility, with two bulky pentaphenylphenyl groups placed *ortho* to each other, rather than *meta* as in compound **1**. If $\Delta G^{\ddagger}_{rac}$ for compound **2** is a mere 4 kcal/mol greater than that observed for **1**, then an enantiomerically pure sample of **2** will be stable for days at room temperature. We report here the synthesis and X-ray structure of compound **2**, as well as two methoxy-substituted derivatives, and the determination of the $\Delta G^{\ddagger}_{rac}$ for these systems by dynamic NMR spectroscopy.

2. Results and discussion

2.1. Syntheses and structures of compound 2 and its methoxy derivatives

Compound **2** was prepared by the double Diels-Alder addition of tetracyclone (**4**) to 1,2-bis(phenylethynyl)benzene [6] (**3**). At the reaction temperature of 260 °C, the cycloadditions were immediately followed by decarbonylation and dehydrogenation to give **2** in 70% yield (Scheme 1). Single crystals of **2** formed upon evaporation of a solution in $CHCl_3$-CH_2Cl_2, and X-ray analysis gave the molecular structure of **2** illustrated in Fig. 1. The molecule lies on a general position in the crystal, but as expected, it adopts a conformation with approximate C_2 symmetry.

It subsequently proved necessary to prepare methoxy

* Corresponding author.
E-mail address: rpascal@tulane.edu (R.A. Pascal).

https://doi.org/10.1016/j.tet.2019.03.055
0040-4020/

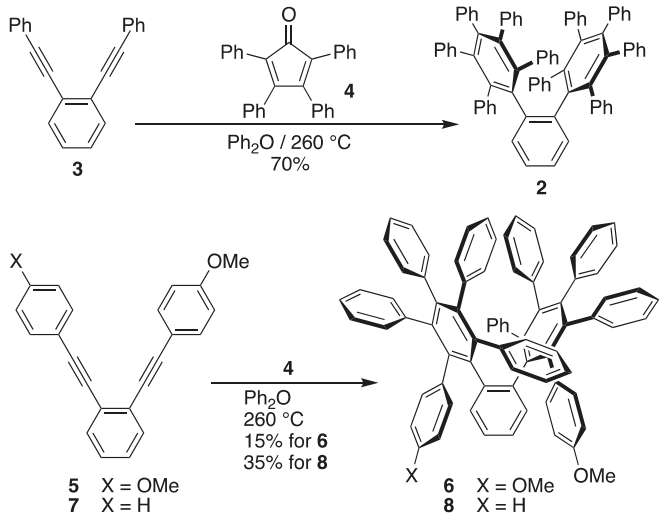

Scheme 1.

derivatives of compound **2** for VT NMR analysis, and the dimethoxy derivative **6** was prepared from 1,2-bis(4-methoxyphenylethynyl)-benzene [7] (**5**) in a manner similar to that used for the parent hydrocarbon (Scheme 1). Single crystals of **6** were obtained from hexanes-CH_2Cl_2, and its molecular structure is also illustrated in Fig. 1. A monomethoxy derivative of **2**, compound **8**, was also prepared by the reaction of tetracyclone with 1-(4-methoxyphenylethynyl)-2-(phenylethynyl)benzene [8] (**7**) as before, but its X-ray structure was not determined.

The structures of compounds **2** and **6** are quite similar, but the steric crowding in both molecules is evident from the large interior angles made by the *ipso* carbons of the pentaphenylphenyl groups and the substituted carbons of the "bottom" benzene rings. Thus, in compound **2**, the angles C(1)-C(6)-C(7) [125.5(1)°] and C(6)-C(1)-C(43) [125.1(1)°] are significantly wider than the standard value of 120°, and in compound **6**, the angles C(1)-C(6)-C(44) [124.7(2)°] and C(6)-C(1)-C(7) [125.0(2)°] are similarly large (the crystallographic numbering schemes in Fig. 1 have been used).

2.2. The free energy of activation for the racemization of compound 2

Hoping for configurational stability, we attempted to resolve compound **2** by both HPLC and supercritical fluid chromatography (SFC) on a wide variety of chiral supports. All of these attempts yielded a single peak for compound **2** with no evidence of even partial resolution. Of course, the failure to resolve compound **2** does not establish that it has a low racemization barrier, but it does suggest that the system should be examined by dynamic NMR spectroscopy at high temperatures or by dynamic chromatography at temperatures at or below 0 °C.

Although the ^{1}H NMR spectrum of compound **2** is sharp at room temperature, one observes broadening and coalescence of various peaks at temperatures ranging from 60 °C to 150 °C (data not shown). Unfortunately, there is no simple way to assign these observations to specific conformational reactions. One may expect not only racemization, but also the rotation of more highly restricted phenyl groups in this range of temperatures.

A simple way to exclude phenyl rotation from consideration is to label compound **2** with *p*-methoxy groups on one or more of the phenyl rings. For this reason we prepared the dimethoxy derivative **6** as shown in Scheme 1. However, compound **6** exists as a mixture of *syn* and *anti* isomers which do not interconvert (we estimate the barrier to be on the order of 45 kcal/mol); they are schematically illustrated in the left panel of Scheme 2. We had hoped to be able to isolate the *syn* isomer (structure **A** and its enantiomer **eA**) and observe the racemization process by VT NMR as a simple coalescence of the two methoxy group resonances. Unfortunately, the *syn* and *anti* isomers proved inseparable in our hands; indeed, as may be seen from the X-ray structure of **6**, they co-crystallize. The *anti* isomer exists as two pairs of enantiomers (**B** and **eB**, and **C** and **eC**), and the "racemization" process actually interconverts the diastereomeric **B** and **eC**, and **C** and **eB** (Scheme 2). This is not an intractable problem, however, because there are only four types of methoxy groups in an achiral environment: the two resonances for the "outside" methoxy group of **A** and the two methoxy groups of **B** are very close (δ 3.736 and 3.741 in $CDCl_3$), as are the two resonances for the "inside" methoxy group of **A** and the two methoxy groups of **C** (δ 3.563 and 3.569). However, one must remember that in a VT NMR experiment, one is observing two distinct processes which conceivably have slightly different barriers.

In the event, the methoxy resonances in **6** were significantly broadened by 130 °C, and coalescence occurred at 150 °C (see the Supporting Information). For an *average* $\Delta\nu = 134$ Hz in the absence of exchange (at 300 MHz in nitrobenzene-d_5), the Gutowsky-Holm approximation gives $k_c = 298$ s^{-1} for coalescence at 150 °C ($T_c = 423$ K). If a transmission coefficient of 1 is assumed for the Eyring equation, then $\Delta G_c^{\ddagger} = 20.3$ kcal/mol [9].

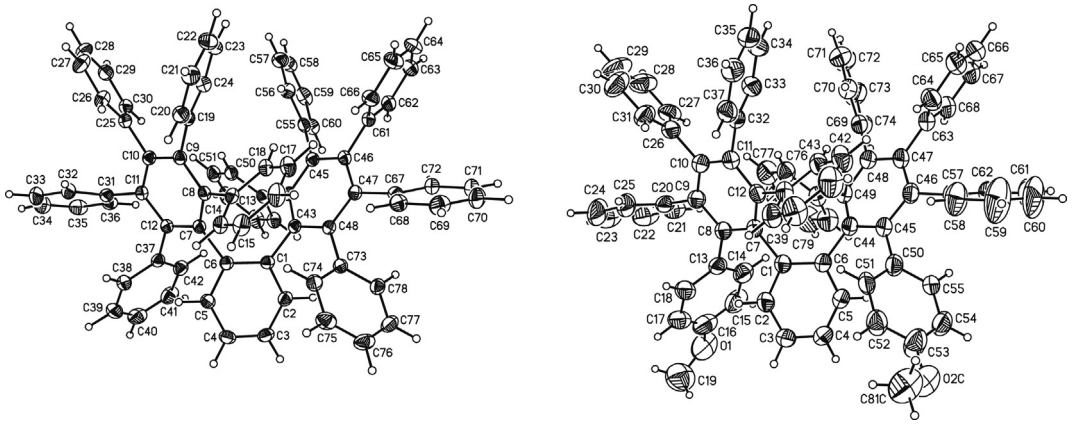

Fig. 1. Molecular structures of compounds **2** (left) and **6** (right). Thermal ellipsoids have been drawn at the 50% probability level. Compound **6** is a disordered mixture of the *syn* and *anti* dimethoxy derivatives in various orientations; only one orientation of the *anti* isomer is illustrated.

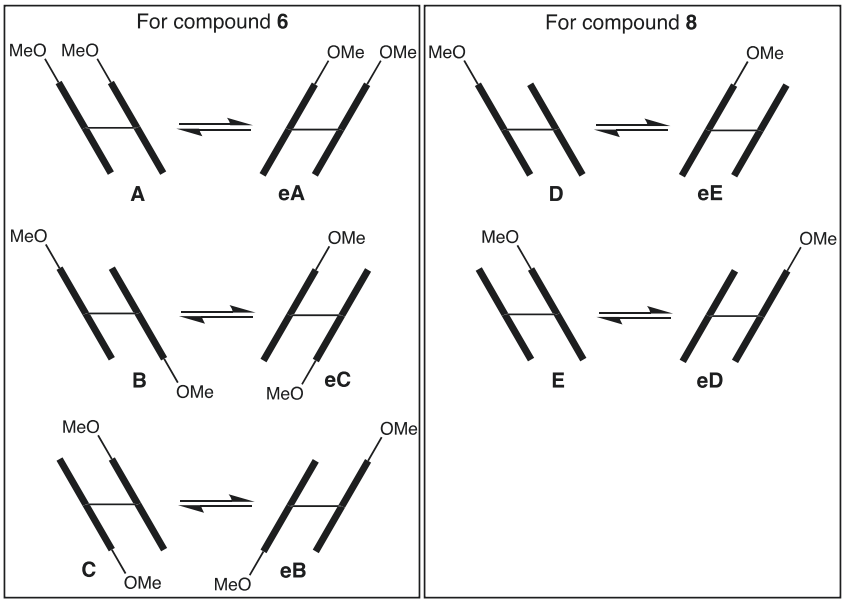

Scheme 2.

Although dynamic NMR is relatively insensitive to small errors in $\Delta\nu$ and T_c, we wished to repeat the experiment with a simpler system. For this reason, the monomethoxy derivative **8** was prepared (Scheme 1). For this molecule, there are only two types of methoxy groups (Scheme 2, right panel), and the "racemization" process actually interconverts the diastereomeric **D** and **eE**, and **E** and **eD**. The variable temperature NMR experiment with **8** very strongly resembles that for **6**, and the methoxy regions of the spectra are illustrated in Fig. 2 (the full spectra, with additional temperatures, are found in the Supporting Information). As before, coalescence occurs at 150 °C. For $\Delta\nu = 135$ Hz in the absence of exchange (at 300 MHz in nitrobenzene-d_5), the Gutowsky-Holm approximation gives $k_c = 300\ s^{-1}$ for coalescence at 150 °C ($T_c = 423$ K). If a transmission coefficient of 1 is assumed for the Eyring equation, then $\Delta G^{\ddagger}_{c} = 20.3$ kcal/mol [9].

The VT NMR data for both **6** and **8** indicate that $\Delta G^{\ddagger}_{rac} = 20.3$ kcal/mol, and given that the methoxy groups are very unlikely to affect the barrier significantly, the barrier for compound **2** should be the same. It is worth noting that an error of 10 °C for T_c would change the barrier by only 0.5 kcal/mol, and an error of 50 Hz in $\Delta\nu$ would change the barrier by only 0.3 kcal/mol.

2.3. Low temperature chromatography of compounds 2 and 8

The experimental free energy of racemization of 20.3 kcal/mol, measured by dynamic NMR at 150 °C, should be high enough for a

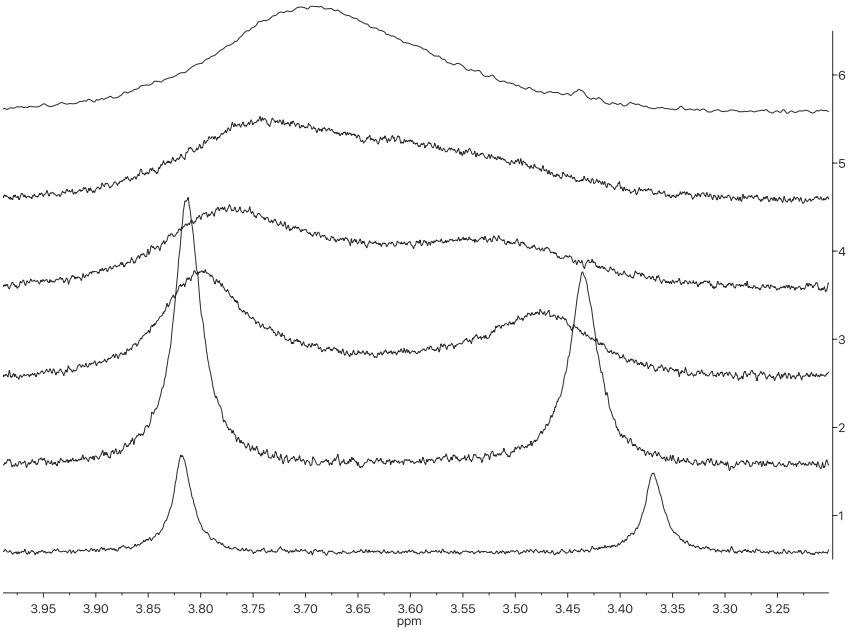

Fig. 2. Variable temperature ^{1}H NMR spectra (300 MHz, nitrobenzene-d_5) of compound **8** (methoxy region). Spectrum 1, 25 °C; 2, 100 °C; 3, 135 °C; 4, 145 °C; 5, 150 °C; 6, 160 °C.

measurement by dynamic chromatography at *ca.* 0 °C, where such a barrier corresponds to a half-life of about 30 min. Compounds **2** and **8** were subjected to HPLC at 0 °C on a variety of chiral supports (Chiralcel OD, Chiralcel OJ, Chiralcel OZ-H, Chiralpak AD, Chiralpak IG, and Whelk-O1(R,R)) using a variety of solvent systems (MeOH, 1:1 MeOH-acetonitrile, and 1:1 hexanes-EtOH), but in all cases only a single, symmetric peak was observed. Unfortunately, this result is inconclusive. Either the isomers do not separate under these conditions, or the racemization barrier is a bit lower than 20 kcal/mol at 0 °C. The measurement of a barrier of even 19 kcal/mol would be difficult at 0 °C, and in the past we encountered serious problems with solvent viscosity when operating at temperatures below 0 °C.

2.4. Computational studies of the racemization of compound 2

At the B3LYP/6-31G(d) level of theory previously employed for compound **1** [1], compound **2** possesses a C_2-symmetric lowest energy conformation resembling the conformations observed in the X-ray structures of **2** and **6**. We initially hypothesized that the transition state structure for racemization might possess C_{2v} symmetry, but after geometry optimization and analytical frequency calculations, all the C_{2v} conformations examined were found to display two or more imaginary frequencies. When the symmetry was lowered to C_s, however, a genuine transition state structure (one imaginary frequency) for racemization was easily located. The B3LYP/6-31G(d)-calculated C_2 minimum and C_s transition state structures are illustrated in Fig. 3. The calculated free energies of activation for racemization ($\Delta G^{\ddagger}_{rac}$, the **bold** values in Table 1) at this level are 18.4 kcal/mol at 298 K and 17.9 kcal/mol at 423 K (the latter is the coalescence temperature in the VT NMR experiments), only 2 kcal/mol lower than the experimental values.

We might have been satisfied with this result, but in a previous study of the racemization of a polyaryl cyclophane [10], the inclusion of dispersion corrections, specifically the D3 correction of Grimme [11], was found to improve slightly the calculated barrier. We therefore repeated the calculations at the B3LYP-D3/6-31G(d) level. The minimum energy structure still possesses C_2 symmetry, but the C_s conformation now displays two imaginary frequencies; thus, it is not a genuine transition state (see Table 1). A transition state search in the absence of symmetry constraints gave a C_1-symmetric transition state structure, and this is also illustrated in Fig. 3.

The inclusion of dispersion corrections in the calculation causes the pentaphenylphenyl "wings" of compound **2** to pack more closely in both the ground state and transition state structures than in the uncorrected calculations, an obvious result of the increased van der Waals attraction. A simple measure of this compression is the distance C9-C19 in the computed structures (see Fig. 3). Thus, for example, in the calculated ground state structures, the C9-C19 distances are 6.528 Å and 6.382 Å for the B3LYP and B3LYP-D3 methods, respectively. In the X-ray structure, this distance is 6.503 Å. A more significant effect of the inclusion of dispersion corrections is an unreasonably large increase in the calculated $\Delta G^{\ddagger}_{rac}$'s: 26.6 kcal/mol at 298 K and 26.5 kcal/mol at 423 K. If these values were correct, then **2** would be configurationally stable at room temperature, but, alas, it is not.

Dispersion corrections for (mainly) DFT calculations are very popular and rapidly evolving [12]. In 2011, Goerigk and Grimme benchmarked DFT methods against their GMTKN30 database [13], and in this study, the D3 correction was employed almost exclusively. However, in their more recent (2017), more extensive, benchmarking paper employing their larger GMTKN55 database [14], the authors recommend that the D3 correction with Becke-Johnson damping [15] ["D3(BJ)"] be employed, except in the case of the Minnesota functionals (e.g. M052X [16] and M062X [17]), where the D3(BJ) correction yields undesirable "short-range double-counting" effects [14]. In the 2011 study, the M062X-D3 functional gave the best overall results among hybrid functionals tested, and in the 2017 study, the M052X-D3 functional was second-best among hybrid functionals (the very slightly better wB97X-D3 was not available for this study). Our own experience with hybrid DFT calculations suggests that B3PW91 [4a,18] is the best of the older hybrid functionals for calculations of structures [19] and hydrocarbon energies [20].

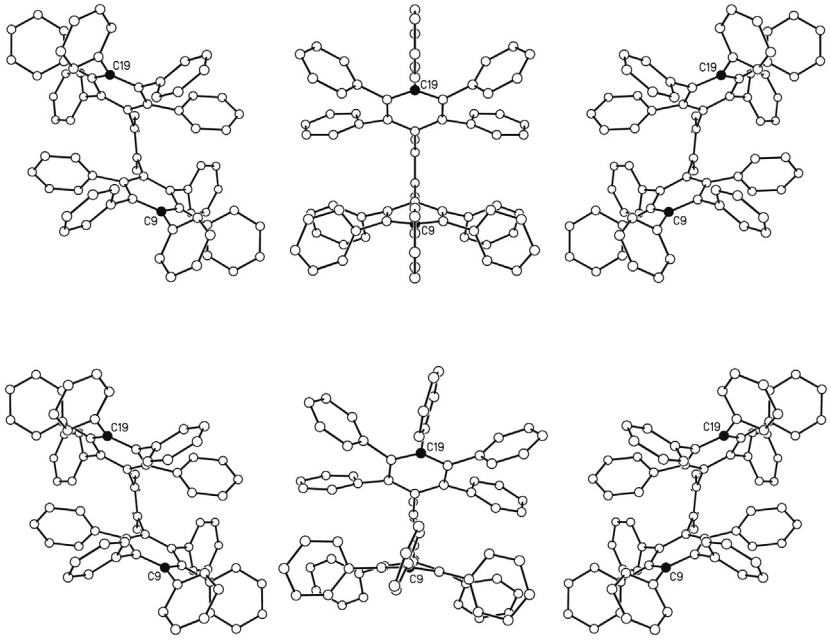

Fig. 3. Calculated minimum energy and racemization transition state structures for compound **2**. Top row: C_2 minimum, C_s transition state, and enantiomeric C_2 minimum calculated at the B3LYP/6-31G(d) level of theory. Bottom row: C_2 minimum, C_1 transition state, and enantiomeric C_2 minimum calculated at the B3LYP-D3/6-31G(d) level of theory.

Table 1
Calculated racemization barriers for 1,2-bis(pentaphenylphenyl)benzene (**2**).

Method	Symm	E + ZPE	$\Delta(E$ + ZPE)	G_{298}	ΔG_{298}	nI[b]	G_{423}	ΔG_{423}
		(au)[a]	(kcal/mol)	(au)[a]	(kcal/mol)		(au)[a]	(kcal/mol)
B3LYP/6-31G(d)	C_2	−3003.754938	0.0	−3003.854983	0.0	0	−3003.933531	0.0
B3LYP/6-31G(d)	C_s	−3003.723174	19.9	−3003.825690	**18.4**	1	−3003.904951	**17.9**
B3LYP-D3/6-31G(d)	C_2	−3003.976297	0.0	−3004.074297	0.0	0	−3004.151713	0.0
B3LYP-D3/6-31G(d)	C_s	−3003.932345	27.6	−3004.030838	27.3	2		
B3LYP-D3/6-31G(d)	C_1	−3003.932679	27.4	−3004.031944	**26.6**	1	−3004.109497	**26.5**
M062X-D3/6-31G(d)	C_2	−3002.586994	0.0	−3002.683897	0.0	0	−3002.760518	0.0
M062X-D3/6-31G(d)	C_s	−3002.536343	31.8	−3002.631885	32.6	2		
M062X-D3/6-31G(d)	C_1	−3002.536782	31.5	−3002.633537	**31.6**	1	−3002.709705	**31.9**
M052X-D3/6-31G(d)	C_2	−3003.601759	0.0	−3003.699379	0.0	0	−3003.776270	0.0
M052X-D3/6-31G(d)	C_s	−3003.553108	30.5	−3003.650669	30.6	2		
M052X-D3/6-31G(d)	C_1	−3003.553368	30.4	−3003.654231	**28.3**	1	−3003.732154	**27.7**
M052X-D3/6-31G(d) PCM[c]	C_2	−3003.627910	0.0	−3003.727456	0.0	0	−3003.805299	0.0
M052X-D3/6-31G(d) PCM[c]	C_s	−3003.583455	27.9	−3003.679843	29.9	2		
M052X-D3/6-31G(d) PCM[c]	C_1	−3003.583684	27.8	−3003.683126	**27.8**	1	−3003.760396	**28.2**
B3PW91/6-311G(d,p)	C_2	−3003.247779	0.0	−3003.347196	0.0	0	−3003.425469	0.0
B3PW91/6-311G(d,p)	C_s	−3003.213568	21.5	−3003.317089	**18.9**	1	−3003.396843	**18.0**
B3PW91-D3(BJ)/6-311G(d,p)	C_2	−3003.717535	0.0	−3003.816807	0.0	0	−3003.894739	0.0
B3PW91-D3(BJ)/6-311G(d,p)	C_s	−3003.664842	33.1	−3003.760634	35.2	3		
B3PW91-D3(BJ)/6-311G(d,p)	C_1	−3003.665116	32.9	−3003.763113	**33.7**	1	−3003.840060	**34.3**
B3PW91/cc-pVTZ	C_2	−3003.531396	0.0	−3003.630976	0.0	0	−3003.709246	0.0
B3PW91/cc-pVTZ	C_s	−3003.500348	19.5	−3003.603323	**17.4**	1	−3003.682758	**16.6**
B3PW91-D3(BJ)/cc-pVTZ	C_2	−3003.999113	0.0	−3004.094541	0.0	0	−3004.170313	0.0
B3PW91-D3(BJ)/cc-pVTZ	C_s	−3003.950137	30.7	−3004.044880	31.2	3		
B3PW91-D3(BJ)/cc-pVTZ	C_1	−3003.950334	30.6	−3004.050436	**27.7**	1	−3004.128208	**26.4**

[a] 1 au = 627.503 kcal/mol.
[b] nI = number of imaginary frequencies.
[c] Solvent: nitrobenzene.

Accordingly, we located the ground state and racemization transition state structures for **2** at the M062X-D3/6-31G(d), M052X-D3/6-31G(d), B3PW91/6-311G(d,p), B3PW91-D3(BJ)/6-311G(d,p), B3PW91/cc-pVTZ, and B3PW91-D3(BJ)/cc-pVTZ levels of theory. The last four calculations, employing larger triple-zeta basis sets, were extremely onerous for so large a molecule as **2**. In each case, the dispersion-corrected DFT methods [M062X-D3, M052X-D3, and B3PW91-D3(BJ)] yielded C_1-symmetric transition state structures with $\Delta G^{\ddagger}_{rac} > 26$ kcal/mol, while the uncorrected B3PW91/6-311G(d,p) and B3PW91/cc-pVTZ calculations gave C_s-symmetric transition states and $\Delta G^{\ddagger}_{rac} \leq 18$ kcal/mol, scarcely different from the much smaller B3LYP/6-31G(d) calculations. In addition, the inclusion of a polarizable continuum solvent model (PCM) for the M052X/6-31G(d) calculation had only a very small effect on the calculated $\Delta G^{\ddagger}_{rac}$.

In response to referees' comments, numerous additional calculations have been placed in the Supplementary Data. These include 13 addition calculations of $\Delta G^{\ddagger}_{rac}$ for compound **2** using a variety of different functionals, both with and without dispersion corrections (Tables S2 and S3), that yield results entirely comparable to those in Table 1. In addition, numerous calculations of the conformational barriers for three smaller hydrocarbons were performed (Table S1). These include the effects of basis set size and composition [using 6-31G(d), 6-31 + G(d), 6-311G(d,p), 6-311++G(2d,p), and cc-pVTZ], the D3 and D3(BJ) dispersion corrections, and the PCM solvent model. The results are compared to the experimental barriers as well as to the results of MP2/cc-pVDZ and CCSD(T)/cc-pVDZ//MP2/cc-pVDZ calculations. Overall, the uncorrected DFT calculations are in better agreement with the experimental and CCSD(T) data, and the effects of basis set size and continuum solvent models are very modest.

That the dispersion-corrected DFT barriers do not match the experimental values is troubling, but could reflect problems beyond the weakness of the models and/or dispersion corrections. Although larger basis sets and continuum solvent models did not provide much help in our tests, calculations including explicit solvent, where *inter*molecular dispersion forces are properly addressed, should give improved results, although at much greater computational cost. Whatever the reason, the problem is no doubt exacerbated by the large area of the interacting surfaces in a molecule the size of **2**, which is much larger than those used to develop and benchmark these computational methods [13,14].

3. Conclusion

The bis(pentaarylphenyl)benzenes **2**, **6**, and **8** were prepared with the hope that these crowded, C_2-symmetric molecules would be configurationally stable and resolvable, given that the much less congested molecular propeller **1** is resolvable at low temperature. Experimentally, however, the free energies of activation for the racemization ($\Delta G^{\ddagger}_{rac}$) of **6** and **8** proved to be only 20.3 kcal/mol, which is 0.5 kcal/mol *lower* than the racemization barrier for **1**. This is presumably due to a destabilization of the ground state conformation by steric crowding, so that the crowded transition state is more easily accessible than one might otherwise expect.

4. Experimental

4.1. General

1,2-Bis(phenylethynyl)benzene (**3**) was prepared by the method of Chen et al. [6], 1,2-bis(4-methoxyphenylethynyl)benzene (**5**) was prepared by the method of Kovalenko et al. [7], and 1-(4-methoxyphenylethynyl)-2-(phenylethynyl)benzene (**7**) was prepared by the method of Peterson et al. [8] All other solvents and reagents were commercial, reagent grade materials, and they were used without further purification. ^{1}H and ^{13}C NMR spectra were recorded at 300 MHz and 75 MHz, respectively, on a Bruker AVANCE 300 spectrometer. Samples were dissolved in $CDCl_3$ for room-temperature spectra and in nitrobenzene-d_5 for the variable temperature NMR studies. High-resolution ESI-TOF mass spectra were recorded on an Agilent 6220 spectrometer.

4.2. Data for compounds

4.2.1. 1,2-Bis(pentaphenylphenyl)benzene (2)

1,2-Bis(phenylethynyl)benzene (**3**, 0.333 g, 1.20 mmol) and tetracyclone (**4**, 1.64 g, 4.3 mmol) were mixed with diphenyl ether (3.5 mL) in a screw-capped Pyrex tube, and the end of the tube was placed in a Wood's metal bath at 260 °C for 48 h. The tube was cooled to room temperature, and the resulting solid was dissolved in CH_2Cl_2. This solution was dropped slowly into stirred methanol (50 mL), and the resulting precipitate was collected by filtration (1.14 g). This solid was mixed with CH_2Cl_2 again, and the undissolved material was collected by filtration to give essentially pure compound **2** (0.837 g, 70%). Single crystals suitable for X-ray analysis were obtained from $CHCl_3$-CH_2Cl_2. ^{1}H NMR (300 MHz, $CDCl_3$) δ 4.56 (d, J = 8 Hz, 2H), 6.22 (m, 4H), 6.43 (m, 8H), 6.61–6.94 (m, 34H), 7.12 (m, 2H), 7.37 (m, 4H); ^{13}C NMR (75 MHz, $CDCl_3$) δ 123.8, 124.0, 124.7, 124.9, 125.0, 125.5, 125.6, 125.96, 126.03, 126.08, 126.3, 126.4, 126.7, 127.0, 127.3, 130.4, 130.6, 131.0, 131.4, 131.7, 131.8, 132.2, 132.3, 133.3, 134.6, 137.7, 138.6, 139.5, 140.4, 140.6, 140.9, 141.0, 141.2, 141.4, 143.9 (35 resonances observed; 29 to 39 resonances are expected, depending on the freedom of rotation of the phenyl groups); HRMS (ESI-TOF) *m/z* 991.4293 (M + H$^+$), calcd for $C_{78}H_{55}^+$, 991.4299.

4.2.2. 1,2-Bis[2-(4-methoxyphenyl)-3,4,5,6-tetraphenylphenyl] benzene (6)

1,2-Bis(4-methoxyphenylethynyl)benzene (**5**, 0.345 g, 1.02 mmol) and tetracyclone (**4**, 0.791 g, 2.06 mmol) were mixed with diphenyl ether (1.2 mL) in a screw-capped Pyrex tube, and the end of the tube was placed in a Wood's metal bath at 260 °C for 48 h. The tube was cooled to room temperature, and the resulting solid was dissolved in CH_2Cl_2. This solution was dropped slowly into stirred methanol (50 mL), and the resulting precipitate was collected by filtration (0.421 g). This material was fractionated by silica gel column chromatography (solvent: 9:1 hexanes-CH_2Cl_2) to give compound **6** (0.113 g). In addition, some of the product failed to dissolve and remained on the top of the column; collection of this material gave additional pure compound **6** (0.051 g). The combined total was 0.164 g (0.156 mmol, 15.3%). Single crystals, suitable for X-ray analysis, were obtained from hexanes-CH_2Cl_2. ^{1}H NMR (300 MHz, $CDCl_3$) δ 3.563 (s, 1.5H), 3.569 (s, 1.5H), 3.736 (s, 1.5H), 3.741 (s, 1.5H), 4.46 (dd, J = 8.5 Hz, 2 Hz, 0.5H), 4.54 (d, J = 8 Hz, 0.5H), 4.66 (dd, J = 8.5 Hz, 2 Hz, 0.5H), 4.73 (d, J = 8 Hz, 0.5H), 5.97 (m, 1H), 6.11 (dd, J = 8.5 Hz, 2 Hz, 1H), 6.25 (m, 5H), 6.44 (m, 7H), 6.60–6.95 (m, 33H), 7.11 (m, 1H), 7.25 (m, 0.5H), 7.35 (m, 1.5H); ^{13}C NMR (126 MHz, $CDCl_3$) δ 54.89, 54.91, 55.26, 55.27, 110.9, 111.0, 111.3, 111.4, 112.4, 113.5, 123.76, 123.83, 123.86, 123.94, 124.0, 124.1, 124.57, 124.58, 124.64, 124.90, 124.91, 124.94, 124.99, 125.4, 125.5, 125.6, 125.7, 125.9, 125.96, 125.98, 126.06, 126.12, 126.2, 126.33, 126.36, 126.38, 126.44, 126.7, 126.9, 127.0, 127.27, 127.31, 130.4, 130.5, 130.6, 130.7, 130.9, 130.0, 131.0, 131.43, 131.46, 131.51, 131.72, 131.77, 131.79, 131.85, 131.89, 131.93, 131.96, 132.16, 132.24, 132.27, 132.33, 132.37, 133.10, 133.19, 133.25, 133.30, 133.33, 133.90, 133.92, 134.16, 134.23, 134.6, 137.9, 138.0, 138.68, 138.72, 138.76, 138.78, 139.07, 139.09, 139.4, 139.5, 140.2, 140.3, 140.42, 140.44, 140.69, 140.71, 140.86, 140.88, 140.97, 141.03, 141.06, 141.12, 141.25, 141.29, 141.32, 141.5, 143.5, 143.6, 143.8, 143.9, 156.38, 156.43, 157.86, 157.89 (108 resonances observed; 120 resonances are expected for two isomers with fast phenyl rotation); HRMS (ESI-TOF) *m/z* 1051.4511 (M + H$^+$), calcd for $C_{80}H_{59}O_2^+$, 1051.4515.

4.2.3. 1-[1-(4-methoxyphenyl)-2,3,4,5-tetraphenylphenyl]-2-(pentaphenylphenyl)benzene (8)

1-(4-methoxyphenylethynyl)-2-(phenylethynyl)benzene (**7**, 0.536 g, 1.74 mmol) and tetracyclone (1.40 g, 3.63 mmol) were mixed with diphenyl ether (1 mL) in a screw-capped Pyrex tube, and the end of the tube was placed in a Wood's metal bath at 260 °C for 72 h. The tube was cooled to room temperature, and the resulting solid was dissolved in CH_2Cl_2. This solution was dropped slowly into stirred methanol (150 mL), and the resulting precipitate was collected by filtration (0.836 g). This material was fractionated by silica gel column chromatography (solvent, 9:1 hexanes-CH_2Cl_2) to give pure compound **8** (0.616 g, 0.604 mmol, 35%). ^{1}H NMR (300 MHz, $CDCl_3$) δ 3.56 (s, 1.5H), 3.74 (s, 1.5H), 4.48 (dd, J = 8.5 Hz, 2 Hz, 0.5H), 4.56 (d, J = 8 Hz, 1H), 4.76 (d, J = 8 Hz, 0.5H), 5.96 (dd, J = 8.5 Hz, 2.5 Hz, 0.5H), 6.13 (dd, J = 8.5 Hz, 2 Hz, 0.5H), 6.24 (m, 4H), 6.46 (m, 7H), 6.63–6.95 (m, 34H), 7.12 (m, 1.5H), 7.29 (dd, J = 8.5 Hz, 2 Hz, 0.5H), 7.37 (m, 3H); ^{13}C NMR (75 MHz, $CDCl_3$) δ 54.9, 55.3, 110.9, 111.4, 112.4, 113.5, 123.76, 123.84, 123.86, 123.95, 124.00, 124.04, 124.14, 124.6, 124.7, 124.92, 124.95, 124.99, 125.5, 125.6, 125.7, 125.9, 125.98, 126.02, 126.09, 126.3, 126.4, 126.5, 126.7, 126.97, 127.01, 127.3, 130.3, 130.4, 130.5, 130.6, 130.7, 130.9, 131.0, 131.39, 131.45, 131.49, 131.71, 131.76, 131.85, 131.91, 132.16, 132.19, 132.26, 132.32, 133.1, 133.19, 133.23, 133.3, 133.9, 134.2, 134.6, 134.7, 137.8, 137.9, 138.0, 138.55, 138.56, 138.76, 138.83, 139.1, 139.46, 139.49, 140.3, 140.4, 140.5, 140.6, 140.70, 140.72, 140.87, 140.91, 140.97, 140.98, 141.02, 141.11, 141.19, 141.20, 141.27, 141.30, 141.4, 141.5, 143.6, 143.89, 143.91, 143.9, 156.4, 157.9 (92 resonances observed, 118 resonances are expected for two isomers with fast phenyl rotation); HRMS (ESI-TOF) *m/z* 1021.4404 (M + H$^+$), calcd for $C_{79}H_{57}O^+$, 1021.4404.

4.3. Computational methodology

All density functional calculations were performed with Gaussian 09, revisions A.02 and D.01 [21]. The built-in default thresholds for integral accuracy, and wave function and gradient convergence were employed for all reported calculations. Transition state structures were located by means of the QST3 program option or by optimization under a symmetry constraint. All potential minima and transition states were verified by analytical frequency calculations at the same level of theory as the geometry optimizations.

Acknowledgment

This work was supported in part by National Science Foundation Grants CHE-1265507, CHE-1762452, and MRI-1228232, and Louisiana Board of Regents Grant LEQSF-(2002-03)-ENH-TR-67 (the latter two for instrumentation in the Tulane X-ray diffraction facility).

Appendix A. Supplementary data

Supplementary data to this article can be found online at https://doi.org/10.1016/j.tet.2019.03.055.

References

[1] R.A. Pascal Jr., C.M. Kraml, N. Byrne, F.J. Coughlin, Tetrahedron 63 (2007) 11902–11910.
[2] M.J.S. Dewar, E.G. Zoebisch, E.F. Healy, J.J.P. Stewart, J. Am. Chem. Soc. 107 (1985) 3902–3909.
[3] W.J. Hehre, L. Radom, P. v. R. Schleyer, J.A. Pople, Ab Initio Molecular Orbital Theory, John Wiley & Sons, New York, 1986, pp. 63–100.
[4] (a) A.D. Becke, J. Chem. Phys. 98 (1993) 5648–5652;
(b) C. Lee, W. Yang, R.G. Parr, Phys. Rev. B 37 (1988) 785–789;
(c) B. Miehlich, A. Savin, H. Stoll, H. Preuss, Chem. Phys. Lett. 157 (1989) 200–206.
[5] O. Trapp, Chirality 18 (2006) 489–497.
[6] C. Chen, M. Harhausen, R. Liedtke, K. Bussman, A. Fukazawa, S. Yamaguchi, J.L. Peterson, C.G. Daniliuc, R. Fröhlich, G. Kehr, G. Erker, Angew. Chem. Int. Ed. 52 (2013) 5992–5996.

[7] S. Kovalenko, S. Peabody, M. Manoharan, R. Clark, I. Alabugin, Org. Lett. 6 (2004) 2457–2460.
[8] P.W. Peterson, N. Shevchenko, B. Breiner, M. Manoharan, F. Lufti, J. Delaune, M. Kingsley, K. Kovnir, I. Alabugin, J. Am. Chem. Soc. 138 (2016) 15617–15628.
[9] J. Sandstrom, Dynamic NMR Spectroscopy, Academic, New York, 1982, pp. 77–123.
[10] R.A. Pascal Jr., A. Dudnikov, L.A. Love, X. Geng, K.J. Dougherty, J.T. Mague, C.M. Kraml, N. Byrne, Eur. J. Org. Chem. (2017) 4194–4200.
[11] S. Grimme, J. Antony, S. Ehrlich, H. Krieg, J. Chem. Phys. 132 (2010) 154104.
[12] S. Grimme, A. Hansen, J.G. Brandenburg, C. Bannwarth, Chem. Rev. 116 (2016) 5105–5154.
[13] L. Goerigk, S. Grimme, Phys. Chem. Chem. Phys. 13 (2011) 6670–6688.
[14] L. Goerigk, A. Hansen, C. Bauer, S. Ehrlich, A. Najibi, S. Grimme, Phys. Chem. Chem. Phys. 19 (2017) 32184–32215.
[15] A.D. Becke, E.R. Johnson, J. Chem. Phys. 123 (2005) 154101.
[16] Y. Zhao, N.E. Schultz, D.G. Truhlar, J. Chem. Theory Comput. 2 (2006) 364–382.
[17] Y. Zhao, D.G. Truhlar, Theor. Chem. Acta 120 (2008) 215–241.
[18] J.P. Perdew, Y. Wang, Phys. Rev. B 45 (1992) 13244–13249.
[19] R.A. Pascal Jr., J. Phys. Chem. A 105 (2001) 9040–9048.
[20] P.R. Schreiner, A.A. Fokin, R.A. Pascal Jr., A. de Meijere, Org. Lett. 8 (2006) 3635–3638.
[21] Frisch, M. J.; Trucks, G. W.; Schlegel, H. B.; Scuseria, G. E.; Robb, M. A.; Cheeseman, J. R.; Scalmani, G.; Barone, V.; Mennucci, B.; Petersson, G. A.; Nakatsuji, H.; Caricato, M.; Li, X.; Hratchian, H. P.; Izmaylov, A. F.; Bloino, J.; Zheng, G.; Sonnenberg, J. L.; Hada, M.; Ehara, M.; Toyota, K.; Fukuda, R.; Hasegawa, J.; Ishida, M.; Nakajima, T.; Honda, Y.; Kitao, O.; Nakai, H.; Vreven, T.; Montgomery Jr, J. A.; Peralta, J. E.; Ogliaro, F.; Bearpark, M.; Heyd, J. J.; Brothers, E.; Kudin, K. N.; Staroverov, V. N.; Kobayashi, R.; Normand, J.; Raghavachari, K.; Rendell, A.; Burant, J. C.; Iyengar, S. S.; Tomasi, J.; Cossi, M.; Rega, N.; Millam, J. M.; Klene, M.; Knox, J. E.; Cross, J. B.; Bakken, V.; Adamo, C.; Jaramillo, J.; Gomperts, R.; Stratmann, R. E.; Yazyev, O.; Austin, A. J.; Cammi, R.; Pomelli, C.; Ochterski, J. W.; Martin, R. L.; Morokuma, K.; Zakrzewski, V. G.; Voth, G. A.; Salvador, P.; Dannenberg, J. J.; Dapprich, S.; Daniels, A. D.; Farkas, Ö.; Foresman, J. B.; Ortiz, J. V.; Cioslowski, J.; Fox, D. J. Gaussian, Inc., Wallingford CT, 2009.